American Mineralogist, Volume 90, pages 687–694, 2005

Temperature and composition dependence of structural phase transitions in $Ca(Ti_xZr_{1-x})OGeO_4$

RIKKE ELLEMANN-OLESEN AND THOMAS MALCHEREK*

Universität Heidelberg, Mineralogisches Institut, Im Neuenheimer Feld 236, 69120 Heidelberg, Germany

ABSTRACT

The solid solubility of $CaTiOGeO_4$ with $CaZrOGeO_4$ and the structural phase transitions occurring in this solid solution as a function of temperature and composition were examined using in situ high temperature X-ray powder diffraction. Structural phase transitions were identified based on the determination of spontaneous strain. The transition $P2_1/a$-$A2/a$, which is typical for titanite and $CaTiOGeO_4$, was observed in samples with Zr concentrations up to 10%. The addition of Zr destabilizes the ordered $P2_1/a$ phase and T_c decreases accordingly. The aristotype structure of titanite in space group symmetry $A2/a$ was observed for intermediate compounds. Compounds with high Zr contents exhibit a triclinically distorted titanite structure. Their structure was modeled in space group $A\bar{1}$. The triclinic structure appears at Zr contents of about 70% with T_c close to ambient temperature. Further increase of the Zr content stabilizes the triclinic structure and leads to an increase of T_c up to $T_c = 488$ K in $CaZrOGeO_4$.

INTRODUCTION

The structure of $CaZrOGeO_4$ has recently been described as a triclinically distorted titanite structure, which transforms to the titanite aristotype structure near 488 K (Malcherek and Ellemann-Olesen 2005). However, in terms of structural phase transitions the mineral titanite, $CaTiOSiO_4$, is well known for its $P2_1/a$-$A2/a$ phase transition, related to off-centering of the Ti cation within its octahedral oxygen coordination environment. Details of the titanite structure and its displacive phase transitions have been the subject of numerous papers (Speer and Gibbs 1976; Taylor and Brown 1976; Ghose et al. 1991; Bismayer et al. 1992; Salje et al. 1993; Kek et al. 1997; Kunz et al. 2000; Malcherek 2001; Malcherek et al. 2001). Very similar behavior has been observed for the Ge-analogue, $CaTiOGeO_4$ (Ellemann-Olesen and Malcherek 2005). In these materials the displacive phase transition is characterized by displacement of the titanium atom from the center of the $[TiO_6]$ octahedron. The ordered low temperature phase exhibits alternating short and long Ti-O bonds along [100], with reversed sense of Ti displacement among adjacent octahedral chains. In the macroscopically disordered form ($A2/a$), Ti is nominally found at the center of the $[TiO_6]$ octahedra. In titanite true $A2/a$ symmetry is suggested to be attained only at a second phase transition at about $T_i = 825$ K, with correlated Ti and Ca displacements persisting in the intermediate regime (Zhang et al. 1997; Kek et al. 1997; Malcherek et al. 1999; Malcherek 2001). Similar behavior is observed in isomorphous compounds and in solid solutions, with Sr substituting for Ca (Ellemann-Olesen and Malcherek, in preparation) or with Ge substituting for Si (Ellemann-Olesen and Malcherek, 2005).

Furthermore it is known that the titanite topology may occur in a triclinically distorted form under certain conditions (Malcherek and Ellemann-Olesen 2005). Examples include the montebrasite-amblygonite series $Li[Al(PO_4)OH]$-$Li[Al(PO_4)F]$ (Groat et al. 1990), the structure of $CaGe_2O_5$ (Aust et al. 1976) or the high-pressure form of malayaite (Rath et al. 2003). The structure of $CaZrOGeO_4$ is topologically identical to the structure of the triclinic high-pressure form of malayaite (Malcherek and Ellemann-Olesen 2005). Similar triclinic to monoclinic phase transitions may occur as a function of temperature, e.g., in $CaGe_2O_5$ at $T_c^* = 714 \pm 3$ K (Malcherek and Bosenick 2004). The present study reports temperature- and composition dependent displacive phase transitions in the solid solution $Ca(Ti_xZr_{1-x})OGeO_4$.

EXPERIMENTAL METHOD

A series of six samples was synthesized by solid-state reaction along the join $Ca(Ti_xZr_{1-x})OGeO_4$ (CTGOx) with $x = 0.95$, 0.90, 0.80, 0.50, 0.20, and 0.10. The stoichiometric starting mixtures were prepared from pure fine-grained powders of $CaCO_3$, TiO_2, ZrO_2, and GeO_2 in an open platinum crucible at a maximum temperature of 1323 K. Approximately 2.5 g of starting oxides were ground, pressed into pellets, and heated for several intervals of 5 days with intermittent grindings. The final reactions of the pressed oxide pellet at 1588 K were carried out in a welded Pt-tube to avoid GeO_2 loss. Phase purity of the resulting product was established by powder diffraction analysis. The impurity phases ZrO_2 (baddeleyite, ca. 0.5 wt%) and $CaGe_2O_5$ (ca. 0.8 wt%) were identified in CTGO10. No secondary phases were observed for the remaining compositions.

In situ X-ray powder diffraction measurements up to 1073 K were carried out with an Anton Paar HTK 1200 furnace mounted on a Philips Xpert diffractometer with monochromatic Cu$K\alpha_1$ radiation. Diffraction patterns were recorded in the range 17–90° 2θ using a proportional counter with 4 s/step counting time and a step size of 0.02°. Additional room-temperature powder diffraction data in the range of 5–100° 2θ were obtained from CTGO10 and CTGO20 using a Philips Xpert diffractometer with Cu$K\alpha$ radiation and a secondary beam monochromator. Lattice parameters at elevated temperatures were determined using the LeBail method as implemented in the GSAS program (Larson and Von Dreele 1994). As far as the LeBail analysis is concerned, the compositions CTGO95, CTGO90, CTGO80, and CTGO50 were refined in space group $A2/a$. The $A2/a$ setting was chosen as the superstructure reflections with $k + l = 2n + 1$ are weak and mostly overlapping with the fundamental reflections (Malcherek 2001). For compositions CTGO20 and CTGO10 the $A\bar{1}$ space group was chosen. Rietveld refinements were carried out using the room temperature data only. For the Rietveld refinement $P2_1/a$ symmetry was used for compositions CTGO95 and CTGO90 and the $A2/a$ symmetry for CTGO80 and CTGO50. Triclinic compounds were refined using space group $A\bar{1}$ with starting parameters from $CaZrOGeO_4$ (Malcherek and Ellemann-Olesen 2005). The isotropic thermal parameters of the oxygen atoms had to be constrained to the same value to obtain positive definite thermal parameters

* E-mail: tmalch@min.uni-heidelberg.de

0003-004X/05/0004–687$05.00/DOI: 10.2138/am.2005.1767

for all atoms. Starting coordinates for monoclinic compounds were taken from the known structure of $CaTiOGeO_4$.

The variation of the shape and size of the unit cell as a result of the phase transition is expressed in terms of the spontaneous strain. The components of the strain tensor were calculated according to the equations given by Carpenter et al. (1998). In the following we will distinguish symmetry breaking (sb) strain components, i.e., e_{12} and e_{23}, from non-symmetry breaking (nsb) components. The scalar spontaneous strain is defined as

$$e_s = (\sum e_{ij}^2)^{1/2}$$

In the case of a zone center transition, the sb-strain, which usually contributes most to the scalar strain defined above, should be proportional to the driving order parameter of the transition. If the critical point is located at the zone boundary of the first Brillouin zone of the high symmetry phase, the scalar strain should be proportional to the square of the order parameter, Q^2, as is the case for the $P2_1/a$-$A2/a$ transition in titanite. Details regarding the coupling of order parameter and spontaneous strain can be found in Carpenter et al. (1998) and Salje (1990).

RESULTS

The compounds $CaZrOGeO_4$ and $CaTiOGeO_4$ form a solid solution for all investigated compositions under the conditions of synthesis applied here. Rietveld refinements were carried out for all room temperature data. The resulting ambient temperature lattice constants are given in Table 1. The refinements reveal a high sensitivity of the crystal symmetry to the amount of Zr present. Across the solid solution the replacement of Ti by the larger Zr atom leads to a gradual increase in cell volume by 9%. A decrease in the monoclinic angle β is seen as the Ti-content decreases. The *a*-, *b*-, and *c*-lattice parameters increase across the solid solution toward the $CaZrOGeO_4$ end-member. The compositional variation of the *a*- and *b*-lattice parameters is linear irrespective of the crystal symmetry at room temperature while the *c* parameter shows a minor change in slope depending on the actual structure. The deviation of the α and γ angles from 90° indicates the compositionally induced phase transition (Fig. 1). Lattice constants as a function of temperature for all intermediate compounds are listed in Table 2. By extrapolation of the lattice parameters measured for $T \geq 538$ K toward lower temperatures, linear reference functions of thermal expansion were obtained for all lattice parameters. These thermal expansion data were used to calculate the strain components.

The refined structural parameters at room temperature are given in Table 3. The variation of the mean bond lengths is displayed in Table 4. As expected the bond lengths of the octahedral cation to the surrounding oxygen atoms increase linearly with increasing Zr content. The mean Ge-O bond distance is constant within the limits of the measurement accuracy. The mean bond length of Ca to the surrounding oxygen atoms is constant but with a marked step between the monoclinic and triclinic compounds caused by the change in Ca-coordination. The mean [8]Ca-O bond length is 2.57 Å in the triclinic phases, whereas the [7]Ca-O bond length is 2.47 Å in the Ti end-member (Fig. 2). Bond valence sums are given in Table 5.

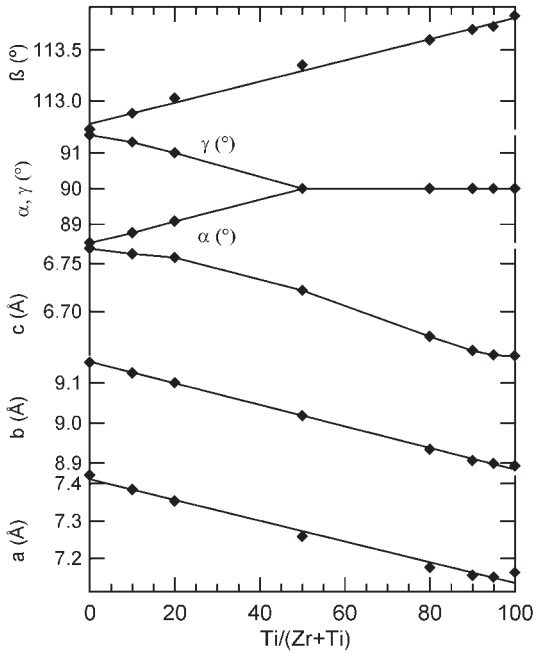

FIGURE 1. $Ca(Ti_xZr_{1-x})OGeO_4$. Lattice constants as a function of Ti content at room temperature.

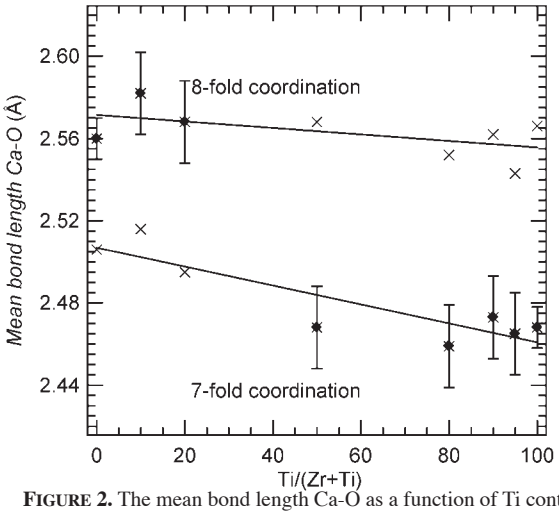

FIGURE 2. The mean bond length Ca-O as a function of Ti content. The dashed lines are calculated mean bond-lengths for Ca in seven- and eightfold coordination extended into the triclinic and monoclinic phases, respectively.

TABLE 1. Lattice parameters for $Ca(Ti_xZr_{1-x})OGeO_4$ at room temperature

Mol% Ti	*a* (Å)	*b* (Å)	*c* (Å)	α (°)	β (°)	γ (°)	*V* (Å³)
100	7.16144(6)	8.89229(2)	6.65311(4)	90	113.833(1)	90	387.552(5)
95	7.15000(6)	8.89941(1)	6.65482(4)	90	113.730(1)	90	387.649(6)
90	7.15461(8)	8.90612(7)	6.65901(5)	90	113.701(1)	90	388.523(7)
80	7.17490(1)	8.93321(4)	6.67312(1)	90	113.600(1)	90	391.940(7)
50	7.25821(3)	9.01791(2)	6.72200(1)	90	113.351(1)	90	403.944(6)
20	7.35292(2)	9.10000(7)	6.75633(7)	89.085(1)	113.024(1)	91.001(1)	415.981(6)
10	7.38422(2)	9.12413(7)	6.76031(1)	88.765(1)	112.877(1)	91.297(1)	419.499(6)
0	7.42260(1)	9.1508(1)	6.7657(1)	88.482(1)	112.719(1)	91.502(1)	423.68(1)

Notes: Data for $CaTiOGeO_4$ and $CaZrOGeO_4$ are taken from Ellemann-Olesen and Malcherek 2005 and Malcherek and Ellemann-Olesen 2005, respectively.

TABLE 2. $Ca(Ti_xZr_{1-x})OGeO_4$. Lattice constants and volume for all intermediate samples as a function of temperature

Mol% Ti	T (K)	a (Å)	b (Å)	c (Å)	β (°)	V (Å³)
95	298	7.15000(6)	8.89941(8)	6.65482(4)	113.730(1)	387.649(6)
	348	7.15000(6)	8.90215(9)	6.65564(3)	113.723(2)	387.859(8)
	373	7.15099(5)	8.90306(2)	6.65651(4)	113.707(2)	388.098(7)
	398	7.15147(5)	8.90598(2)	6.65732(2)	113.698(1)	388.340(4)
	423	7.15173(3)	8.90846(4)	6.65867(5)	113.688(1)	388.526(5)
	448	7.15202(5)	8.91033(9)	6.66001(8)	113.686(1)	388.669(7)
	473	7.15239(8)	8.91111(5)	6.66036(7)	113.680(1)	388.761(7)
	498	7.15261(9)	8.91365(5)	6.66124(4)	113.670(1)	388.965(7)
	523	7.15315(3)	8.91536(5)	6.66175(3)	113.659(1)	389.131(4)
	538	7.15353(6)	8.91659(2)	6.66263(7)	113.654(2)	389.272(8)
	553	7.15372(8)	8.91742(4)	6.66265(2)	113.655(1)	389.317(6)
	573	7.15424(4)	8.91947(6)	6.66449(7)	113.652(1)	389.551(6)
	598	7.15449(2)	8.92113(9)	6.66527(8)	113.647(1)	389.698(7)
	623	7.15546(4)	8.92320(8)	6.66648(7)	113.643(1)	389.924(7)
	648	7.15586(5)	8.92469(6)	6.66713(8)	113.637(1)	390.067(7)
	673	7.15651(7)	8.92677(7)	6.66864(5)	113.631(1)	390.299(6)
	723	7.15748(9)	8.92956(4)	6.66950(2)	113.616(1)	390.569(6)
	748	7.15796(9)	8.93160(8)	6.67063(5)	113.611(1)	390.766(7)
	773	7.15860(3)	8.93359(3)	6.67260(9)	113.618(1)	390.982(6)
90	298	7.15461(8)	8.90612(7)	6.65901(5)	113.701(1)	388.523(7)
	348	7.15468(4)	8.90859(2)	6.65980(8)	113.687(1)	388.721(6)
	373	7.15497(8)	8.91073(3)	6.66000(9)	113.674(2)	388.880(8)
	398	7.15517(3)	8.91222(8)	6.66131(6)	113.665(2)	389.061(8)
	423	7.15569(2)	8.91458(8)	6.66279(3)	113.659(1)	389.296(7)
	448	7.15596(6)	8.91580(7)	6.66349(3)	113.655(1)	389.416(6)
	473	7.15639(5)	8.91762(3)	6.66375(4)	113.643(1)	389.569(5)
	498	7.15696(3)	8.92025(3)	6.66545(7)	113.638(1)	389.831(5)
	523	7.15754(2)	8.92136(7)	6.66590(3)	113.632(1)	389.955(6)
	538	7.15754(8)	8.92295(3)	6.66653(2)	113.632(2)	390.061(7)
	553	7.15784(5)	8.92414(4)	6.66793(2)	113.630(1)	390.217(6)
	573	7.15819(5)	8.92632(6)	6.66916(7)	113.622(1)	390.428(4)
	598	7.15826(2)	8.92795(5)	6.66880(2)	113.614(1)	390.505(5)
	623	7.15900(4)	8.92854(8)	6.66942(3)	113.611(1)	390.616(5)
	648	7.15936(2)	8.93094(5)	6.67102(4)	113.611(1)	390.835(6)
	673	7.16001(9)	8.93234(5)	6.67137(2)	113.603(1)	390.977(6)
	723	7.16057(2)	8.93457(2)	6.67244(3)	113.589(2)	391.209(6)
	748	7.16150(7)	8.93704(8)	6.67424(8)	113.588(1)	391.477(8)
	773	7.16176(2)	8.93881(2)	6.67512(4)	113.577(1)	391.653(4)
80	298	7.17490(8)	8.93321(4)	6.67312(8)	113.600(1)	391.940(7)
	348	7.17427(6)	8.93700(8)	6.67498(5)	113.593(1)	392.202(6)
	373	7.17484(8)	8.93850(3)	6.67604(6)	113.590(2)	392.370(8)
	398	7.17592(3)	8.94170(5)	6.67675(2)	113.584(1)	392.630(4)
	423	7.17641(2)	8.94297(2)	6.67731(4)	113.567(1)	392.796(4)
	448	7.17686(5)	8.94496(3)	6.67833(9)	113.569(1)	392.962(7)
	473	7.17828(8)	8.94717(7)	6.68026(7)	113.563(2)	393.267(9)
	498	7.17918(2)	8.94796(8)	6.68084(4)	113.562(2)	393.389(7)
	523	7.17967(4)	8.95101(2)	6.68256(5)	113.549(1)	393.690(5)
	538	7.17942(8)	8.95152(8)	6.68232(6)	113.553(1)	393.673(7)
	553	7.18041(7)	8.95304(7)	6.68356(6)	113.556(1)	393.858(7)
	573	7.18086(5)	8.95419(3)	6.68400(2)	113.552(1)	393.971(4)
	598	7.18197(5)	8.95543(3)	6.68574(6)	113.546(1)	394.207(6)
	623	7.18290(4)	8.95786(6)	6.68670(2)	113.538(1)	394.446(5)
	648	7.18384(2)	8.96060(5)	6.68769(5)	113.530(1)	394.700(5)
	673	7.18347(4)	8.96246(3)	6.68927(3)	113.531(1)	394.852(4)
	723	7.18547(5)	8.96486(8)	6.69046(4)	113.528(1)	395.147(6)
	748	7.18564(7)	8.96677(3)	6.69148(3)	113.526(1)	395.308(5)
	773	7.18647(6)	8.96934(2)	6.69307(8)	113.523(1)	395.570(7)
50	298	7.25821(3)	9.01791(2)	6.72200(9)	113.351(1)	403.944(6)
	348	7.25921(3)	9.02172(3)	6.72416(7)	113.338(1)	404.340(6)
	373	7.26006(6)	9.02397(7)	6.72523(8)	113.338(1)	404.552(7)
	398	7.26081(8)	9.02528(6)	6.72651(4)	113.335(1)	404.739(6)
	423	7.26162(6)	9.02738(9)	6.72758(5)	113.334(1)	404.946(7)
	448	7.26257(3)	9.02909(6)	6.72914(5)	113.332(1)	405.175(5)
	473	7.26336(2)	9.03144(6)	6.72984(8)	113.329(1)	405.376(6)
	498	7.26426(8)	9.03246(7)	6.73120(2)	113.324(1)	405.570(6)
	523	7.26530(2)	9.03502(5)	6.73269(3)	113.321(1)	405.842(4)
	548	7.26611(2)	9.03649(3)	6.73390(6)	113.321(1)	406.026(5)
	573	7.26664(7)	9.03860(2)	6.73485(9)	113.314(1)	406.229(7)
	598	7.26775(4)	9.04009(2)	6.73602(7)	113.314(1)	406.429(6)
	623	7.26839(8)	9.04191(3)	6.73718(6)	113.308(1)	406.635(7)
	648	7.26965(5)	9.04367(6)	6.73868(9)	113.308(1)	406.875(7)
	673	7.27044(7)	9.04572(3)	6.73987(5)	113.304(1)	407.095(6)
	723	7.27210(5)	9.04928(5)	6.74224(8)	113.300(1)	407.504(7)
	748	7.27322(6)	9.05101(2)	6.74384(5)	113.301(1)	407.738(6)
	773	7.27318(6)	9.05177(5)	6.74447(8)	113.297(1)	407.821(7)

continued on next page

The $P2_1/a$-$A2/a$ transition

The end-member composition $CaTiOGeO_4$ is isostructural to titanite and the displacive $A2/a$-$P2_1/a$ phase transition occurs at $T_c = 588 \pm 4$ K (Ellemann-Olesen and Malcherek 2005). Judging by the strain analysis the $P2_1/a$-$A2/a$ phase transition is also observed in the compounds CTGO95 and CTGO90. The evolution of the lattice parameters is in agreement with $CaTiOGeO_4$ (Ellemann-Olesen and Malcherek 2005). However deviation from the linear thermal expansion data is less significant for the a lattice constant and the β angle compared to titanite and $CaTiOGeO_4$. Figure 3 displays the a parameter for CTGO80, CTGO90, CTGO95, and the end-member composition CTGO.

The X-ray diffraction data indicate the aristotype structure ($A2/a$) in the measured temperature range of CTGO50 and CTGO80. There is no discernable deviation from linear thermal expansion for all lattice constants. From this standpoint the compounds do not show evidence of a structural phase transition above ambient temperature. No measurements were carried out below room temperature.

In agreement with previous investigations of $CaTiOGeO_4$ (Ellemann-Olesen and Malcherek 2005) and titanite (Malcherek 2001), the spontaneous strain due to the $P2_1/a$-$A2/a$ phase transition in CTGO95 is relatively small and dominated by the components e_{11} and e_{13}. The square of the scalar strain e_s^2 extrapolates linearly to zero at $T_c = 480 \pm 5$ K. In analogy with the end-member composition $CaTiOGeO_4$ the linear temperature dependence of e^2_s below the phase transition indicates the close to tricritical character of the transition ($Q^4 \propto T - T_c$).

The $A\bar{1}$-$A2/a$ transition

By analogy to $CaZrOGeO_4$ the samples CTGO10 and CTGO20 exhibit the triclinic $A\bar{1}$ structure at low temperatures.

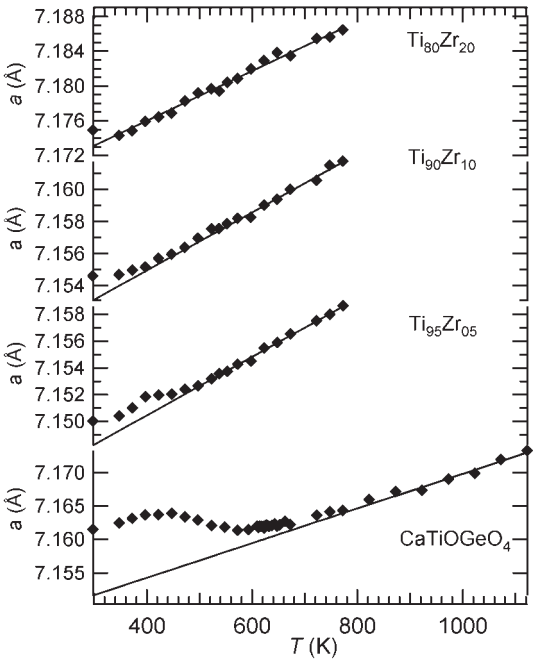

FIGURE 3. The a lattice parameter for CTGO, CTGO95, CTGO90, and CTGO80 as a function of temperature.

TABLE 2. —*Continued*

Mol% Ti								
20	*T* (K)	*a* (Å)	*b* (Å)	*c* (Å)	α (°)	β (°)	γ (°)	*V* (Å³)
	298	7.35292(2)	9.10000(7)	6.75633(7)	89.085(1)	113.024(1)	91.001(1)	415.981(6)
	348	7.35513(5)	9.10561(6)	6.75543(8)	89.570(1)	113.069(1)	90.490(1)	416.848(7)
	373	7.35499(6)	9.10184(6)	6.76906(5)	89.869(1)	113.063(1)	90.136(1)	416.928(6)
	398	7.35792(2)	9.10477(4)	6.77186(3)	90	113.082(1)	90	417.344(4)
	423	7.35814(3)	9.10576(8)	6.77342(4)	90	113.080(1)	90	417.504(6)
	448	7.35896(3)	9.10781(8)	6.77459(2)	90	113.079(1)	90	417.720(5)
	473	7.35960(6)	9.10947(2)	6.77616(8)	90	113.085(1)	90	417.910(7)
	498	7.36089(8)	9.11109(3)	6.77763(7)	90	113.084(1)	90	418.152(7)
	523	7.36146(6)	9.11231(3)	6.77875(3)	90	113.083(1)	90	418.312(6)
	548	7.36266(9)	9.11502(3)	6.78092(7)	90	113.078(1)	90	418.654(8)
	573	7.36371(4)	9.11662(6)	6.78218(8)	90	113.083(1)	90	418.850(7)
	598	7.36381(8)	9.11850(2)	6.78375(2)	90	113.078(1)	90	419.054(6)
	623	7.36537(7)	9.11952(5)	6.78468(6)	90	113.078(1)	90	419.248(7)
	648	7.36578(5)	9.12148(8)	6.78634(6)	90	113.075(1)	90	419.473(7)
	673	7.36700(5)	9.12322(3)	6.78777(7)	90	113.075(1)	90	419.711(6)
	723	7.36833(2)	9.12593(8)	6.79074(8)	90	113.074(1)	90	420.098(7)
	748	7.36904(3)	9.12776(8)	6.79188(7)	90	113.072(1)	90	420.300(7)
	773	7.37016(5)	9.12940(6)	6.79355(8)	90	113.073(1)	90	420.539(7)
10								
	298	7.38422(2)	9.12413(7)	6.76031(1)	88.765(1)	112.877(1)	91.297(1)	419.499(6)
	348	7.38722(9)	9.12970(9)	6.77012(6)	89.009(1)	112.934(1)	91.070(1)	420.408(8)
	373	7.38826(2)	9.12980(9)	6.77625(9)	89.154(1)	112.952(1)	90.902(1)	420.824(8)
	398	7.38970(6)	9.13119(8)	6.78187(4)	89.407(1)	112.967(1)	90.637(1)	421.308(6)
	423	7.39068(8)	9.13331(4)	6.78783(6)	89.785(1)	113.005(1)	90.235(1)	421.744(7)
	448	7.39185(6)	9.13077(9)	6.78910(8)	90	112.993(1)	90	421.814(8)
	473	7.39254(3)	9.13241(5)	6.79062(8)	90	112.991(1)	90	422.030(7)
	498	7.39427(4)	9.13471(2)	6.79201(6)	90	112.996(1)	90	422.306(5)
	523	7.39379(3)	9.13582(7)	6.79356(2)	90	112.994(1)	90	422.433(5)
	548	7.39550(1)	9.13766(5)	6.79524(5)	90	112.995(1)	90	422.717(5)
	573	7.39596(9)	9.13953(2)	6.79671(1)	90	112.995(1)	90	422.921(6)
	598	7.39653(4)	9.14096(1)	6.79794(9)	90	112.988(1)	90	423.118(7)
	623	7.39771(9)	9.14270(9)	6.79952(1)	90	112.992(1)	90	423.352(7)
	648	7.39869(4)	9.14442(1)	6.80099(9)	90	112.992(1)	90	423.580(7)
	673	7.39896(8)	9.14604(1)	6.80220(7)	90	112.985(1)	90	423.767(7)
	723	7.40066(5)	9.14935(2)	6.80521(1)	90	112.990(1)	90	424.190(5)
	748	7.40174(1)	9.15031(1)	6.80653(3)	90	112.988(1)	90	424.385(5)
	773	7.40215(8)	9.15223(6)	6.80798(6)	90	112.987(1)	90	424.591(7)

The evolution of the lattice parameters agrees with that of the end-member composition $CaZrOGeO_4$ (Malcherek and Ellemann-Olesen 2005) (Fig. 4). The triclinic distortion observed at room temperature, as indicated by the deviation of α and γ from 90°, decreases with increasing Ti content.

By linear extrapolation of e_s^2 to zero the transition temperature is estimated to be $T_c = 429 \pm 5$ K and $T_c = 371 \pm 5$ K for CTGO10 and CTGO20, respectively.

The spontaneous strain associated with the triclinic to monoclinic phase transition in the titanite structure is relatively large and is dominated by the symmetry breaking components e_{12} and e_{23} (Fig. 5). For CTGO20 ($T = 298$ K) the e_{23} and e_{12} components are –0.009 and 0.0045, respectively corresponding to a decrease of 33% and 45% from $CaZrOGeO_4$. Therefore the triclinic distortion is lowered by the presence of Ti.

Figure 6 shows the evolution of the non-symmetry breaking strain as a function of reduced temperature. The components e_{13} and e_{33} dominate with symmetrical evolution about the temperature axis. The non-symmetry breaking strain components e_{13} and e_{33} describe a linear contraction of the unit cell approximately parallel to the **c***-direction and simultaneous shearing within the triclinic stability field. As a consequence the volume strain is negative and amounts to –0.19% and –0.27% in CTGO10 and CTGO20, comparable to –0.28% in $CaZrOGeO_4$. The room temperature value of the e_{33} component falls to –0.001 for CTGO20, a decrease of nearly 62% from $CaZrOGeO_4$. As the superposition of the nsb-strain components against reduced temperature demonstrates, the evolution of the nsb-strain is hardly affected by changes in the Ti content, which mainly alters T_c instead (Fig. 6).

A linear dependence is evident between temperature and the square of the scalar strain, e_s^2 (Fig. 7). As the triclinic to monoclinic change in symmetry implies the transition is of the zone center type, it can be concluded that $Q^2 \propto T - T_c$ and the

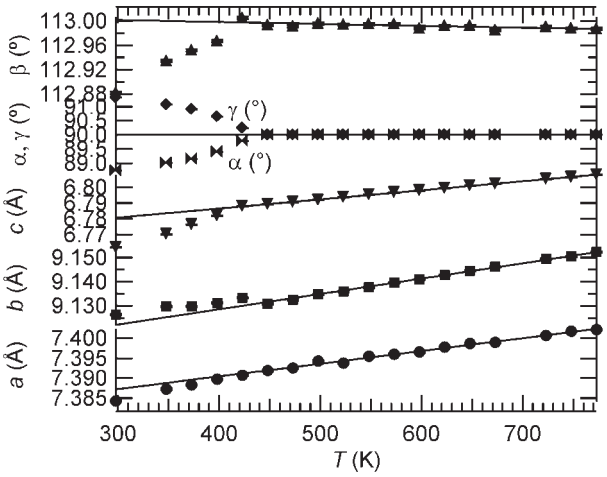

FIGURE 4. Lattice parameters for the compound CTGO10 as a function of temperature. The lines were fitted to the data for $T > 429$ K.

TABLE 3. Atomic positional parameters and isotropic thermal vibration parameters (Å²) at room temperature across $Ca(Ti_xZr_{1-x})OGeO_4$.

Mol% Ti					
95 ($P2_1/a$)	x	y	z	U_{iso}	occ
Ca	0.2413(4)	0.4219(4)	0.2503(2)	0.015(2)	1.000
Ti	0.5027(1)	0.2394(8)	0.7477(2)	0.012(3)	0.954(9)
Zr	0.5027(1)	0.2394(8)	0.7477(2)	0.012(3)	0.046(1)
Ge	0.7488(3)	0.4331(1)	0.2525(4)	0.021(1)	1.000
O1	0.7394(5)	0.3147(3)	0.7684(2)	0.009(4)	1.000
O2A	0.9225(3)	0.3123(8)	0.4287(5)	0.009(4)	1.000
O2B	0.0813(6)	0.1956(7)	0.0457(1)	0.009(4)	1.000
O3A	0.4005(1)	0.4694(3)	0.6430(5)	0.009(4)	1.000
O3B	0.6057(2)	0.0619(4)	0.8656(3)	0.009(4)	1.000
R_P 0.215					
$R(F^2)$ 0.175					
90 ($P2_1/a$)	x	y	z	U_{iso}	occ
Ca	0.2502(7)	0.4223(5)	0.2530(1)	0.013(5)	1.000
Ti	0.5048(8)	0.2422(6)	0.7517(8)	0.019(7)	0.908(6)
Zr	0.5048(8)	0.2422(6)	0.7517(8)	0.019(7)	0.091(4)
Ge	0.7459(7)	0.4332(1)	0.2516(4)	0.025(1)	1.000
O1	0.7400(9)	0.3157(5)	0.7569(1)	0.003(5)	1.000
O2A	0.9261(1)	0.3248(3)	0.4445(1)	0.003(5)	1.000
O2B	0.0996(2)	0.2053(8)	0.0659(9)	0.003(5)	1.000
O3A	0.4146(5)	0.4605(3)	0.6749(9)	0.003(5)	1.000
O3B	0.6154(6)	0.0559(4)	0.8767(3)	0.003(5)	1.000
R_P 0.216					
$R(F^2)$ 0.183					
80 ($A2/a$)	x	y	z	U_{iso}	occ
Ca	0.2500	0.6716(6)	0.5000	0.018(2)	1.000
Ti	0.5000	0.5000	0.0000	0.015(2)	0.807(1)
Zr	0.5000	0.5000	0.0000	0.015(2)	0.192(9)
Ge	0.7500	0.6820(4)	0.5000	0.014(2)	1.000
O1	0.7500	0.5653(9)	0.0000	0.005(3)	1.000
O2A	0.9162(9)	0.5559(6)	0.6887(7)	0.005(3)	1.000
O3A	0.3977(3)	0.7105(9)	0.8934(7)	0.005(3)	1.000
R_P 0.172					
$R(F^2)$ 0.112					
50 ($A2/a$)	x	y	z	U_{iso}	occ
Ca	0.2500	0.6712(4)	0.5000	0.014(3)	1.000
Ti	0.5000	0.5000	0.0000	0.010(1)	0.507(7)
Zr	0.5000	0.5000	0.0000	0.010(1)	0.492(3)
Ge	0.7500	0.6816(2)	0.5000	0.013(2)	1.000
O1	0.7500	0.5695(6)	0.0000	0.009(5)	1.000
O2A	0.9194(8)	0.5539(1)	0.6795(1)	0.009(5)	1.000
O3A	0.3992(4)	0.7204(1)	0.8966(1)	0.009(5)	1.000
R_P 0.135					
$R(F^2)$ 0.0883					
20 $A\bar{1}$	x	y	z	U_{iso}	occ
Ca	0.2329(8)	0.6674(2)	0.5044(8)	0.020(4)	1.000
Ge	0.7495(4)	0.6810(8)	0.4972(1)	0.018(1)	1.000
Ti(1)	0.5	0.5	0.0	0.009(8)	0.222(1)
Ti(2)	0.0	0.5	0.0	0.011(4)	0.222(1)
Zr(1)	0.5	0.5	0.0	0.009(8)	0.778(7)
Zr(2)	0.0	0.5	0.0	0.011(4)	0.778(7)
O1	0.7452(4)	0.5822(1)	0.9973(4)	0.008(2)	1.000
O2A	0.9216(2)	0.5617(8)	0.6757(7)	0.008(2)	1.000
O2B	0.5958(1)	0.5554(3)	0.3329(2)	0.008(2)	1.000
O3A	0.3879(5)	0.7142(7)	0.8923(3)	0.008(2)	1.000
O3B	0.1232(6)	0.7040(5)	0.1283(6)	0.008(2)	1.000
R_P 0.086					
$R(F^2)$ 0.050					
10 $A\bar{1}$	x	y	z	U_{iso}	occ
Ca	0.2289(4)	0.6666(5)	0.5071(6)	0.025(4)	1.000
Ge	0.7481(3)	0.6811(6)	0.4959(6)	0.016(1)	1.000
Ti(1)	0.5	0.5	0.0	0.012(4)	0.114(3)
Ti(2)	0.0	0.5	0.0	0.013(5)	0.114(3)
Zr(1)	0.5	0.5	0.0	0.012(4)	0.885(7)
Zr(2)	0.0	0.5	0.0	0.013(5)	0.885(7)
O1	0.7492(7)	0.5831(7)	0.9941(3)	0.008(2)	1.000
O2A	0.9176(3)	0.5667(2)	0.6739(6)	0.008(2)	1.000
O2B	0.6083(5)	0.5515(3)	0.3273(2)	0.008(2)	1.000
O3A	0.3824(2)	0.7061(6)	0.8947(4)	0.008(2)	1.000
O3B	0.1111(7)	0.6982(5)	0.1128(4)	0.008(2)	1.000
R_P 0.094					
$R(F^2)$ 0.061					

Notes: Data for the endmember compositions $CaTiOGeO_4$ and $CaZrOGeO_4$ see Ellemann-Olesen and Malcherek, 2005 and Malcherek and Ellemann-Olesen, 2005.

transition is continuous second-order in analogy to $CaZrOGeO_4$ (Malcherek and Ellemann-Olesen 2005).

Figure 8 displays the evolution of the critical temperatures as observed by strain analysis across the solid solution.

DISCUSSION

The temperature evolution of the $Ca(Ti_xZr_{1-x})OGeO_4$ solid solution shows a more complicated behavior than previously studied compositions in the titanite structure field (e.g., Kunz et al. 1997; Angel et al. 1999; Ellemann-Olesen and Malcherek 2005). Whereas at high Ti contents the commonly observed $A2/a$-$P2_1/a$ transition is found, a monoclinic to triclinic transition can be observed at high Zr-concentrations. The X-ray diffrac-

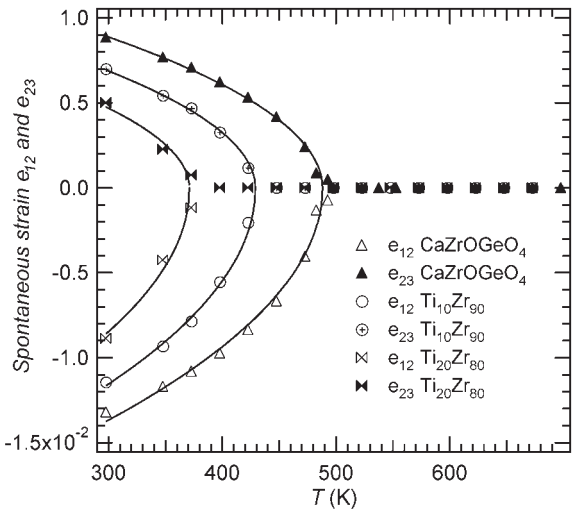

FIGURE 5. Symmetry breaking strain e_{12} and e_{23} for CTGO10, CTGO20, and $CaZrOGeO_4$. The solid curves indicate the temperature behavior given by the Landau model.

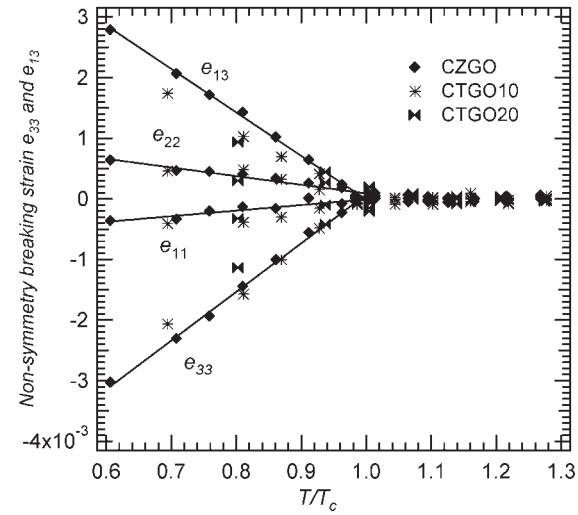

FIGURE 6. The non-symmetry breaking strain components for the triclinic compounds as a function of reduced temperature.

TABLE 4. Mean bond lengths (Å) at room temperature

Mol% Ti	Ge-O	Ti-O	Ca-O
CTGO	1.752	1.964	2.468[7]
95	1.735	1.948	2.460[7]
90	1.767	1.944	2.473[7]
80	1.765	1.969	2.459[7]
50	1.754	2.037	2.469[7]
20	1.750	2.074/2.075	2.496[7], 2.568[8]
10	1.753	2.057/2.045	2.516[7], 2.582[8]
CZGO	1.75	2.11/2.12	2.505[7], 2.559[8]

Notes: Bond lengths for $CaTiOGeO_4$ and $CaZrOGeO_4$ at room temperature are taken from Ellemann-Olesen and Malcherek 2005 and Malcherek and Ellemann-Olesen 2005, respectively.

TABLE 5. Results of bond valence calculations performed at room temperature across the solid solution $Ca(Ti_xZr_{1-x})OGeO_4$. For Ca both in seven- and eightfold coordination

Mol% Ge	CTGO	95	90	80	50	20	10	CZGO
Ge	3.97	4.110	3.878	3.822	3.861	4.007	3.999	4.06
Ti	4.18	4.16	4.15	4.12	4.02	3.92	3.88	–
Zr	–	–	–	–	–	–	–	3.74/3.85
Ca(7)	1.88	1.877	1.920	1.887	1.841	1.795	1.844	1.865
Ca(8)	1.908	1.924	1.900	1.916	1.872	1.894	1.849	1.91

Notes: Bond valence sums were calculated according to Brese and O'Keefe 1991. Data for $CaTiOGeO_4$ and $CaZrOGeO_4$ are taken from Ellemann-Olesen and Malcherek 2005 and Malcherek and Ellemann-Olesen 2005, respectively.

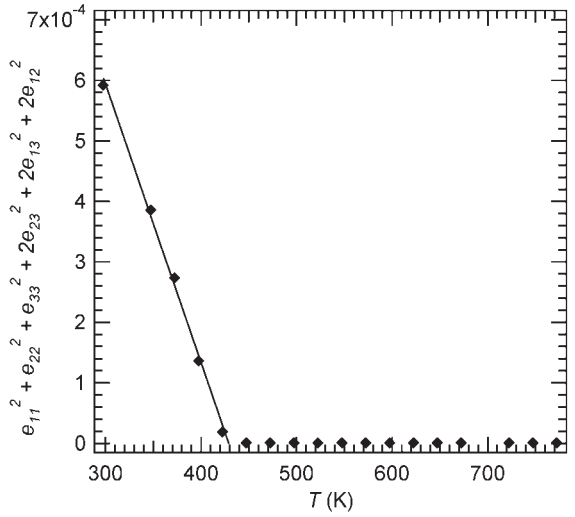

FIGURE 7. CTGO10. The square of the scalar strain, e_s^2, which linearly extrapolates to $T_c = 429$ K.

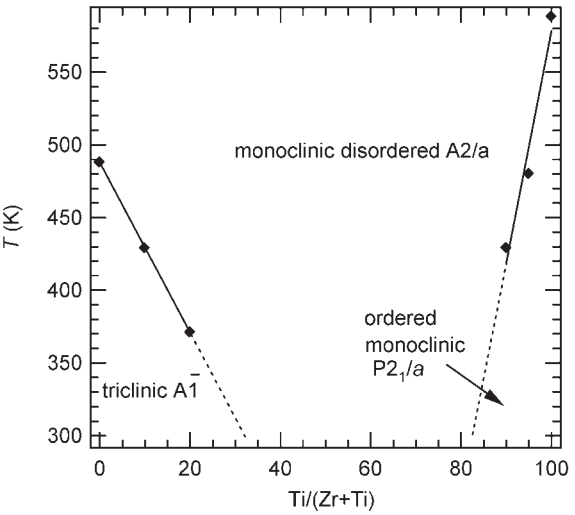

FIGURE 8. The transition temperature as a function of increasing Ti content. The different structure types are listed.

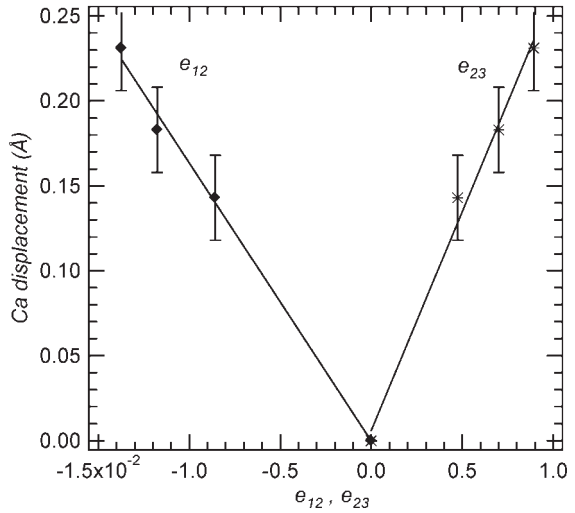

FIGURE 9. Ca displacement as a function of the symmetry-breaking strain components e_{12} and e_{23} at room temperature.

tion data indicate the aristotype structure ($A2/a$) in the measured temperature range for CTGO50 and CTGO80. The compositional range of the triclinic structure is broader than that of the $P2_1/a$ structure. The triclinic-monoclinic compositional phase transition is expected at $Ca(Ti_{32}Zr_{68})OGeO_4$, whereas the transition $P2_1/a$-$A2/a$ occurs at $Ca(Ti_{82}Zr_{18})OGeO_4$. These phase boundaries were estimated from linear extrapolation of the known critical temperatures toward room temperature (Fig. 8).

As a result of the triclinic-monoclinic phase transition, the position of the Ca atom shifts away from the diad axis of the monoclinic phase. The direction of the displacement is approximately parallel to **a**. Figure 9 shows that the Ca displacement at room temperature is a linear function of the symmetry breaking strain components.

In agreement with $CaZrOGeO_4$ the triclinic compounds CTGO10 and CTGO20 show an eightfold coordinated Ca atom when considering the bond distances to all nearest O atoms. The bond valence sums for Ca are 1.849 and 1.894, respectively. This change in coordination is also found in the high-pressure phase transition of malayaite (Rath et al. 2003), in which the observed Ca displacement almost parallel to [100] causes a change in coordination from the originally linear [CaO_7] chains to sheets of [CaO_8] parallel to ($\bar{1}11$). This indicates that the chemically imposed structural strain across $Ca(Ti_xZr_{1-x})OGeO_4$ has a similar effect on the structure as pressure-induced strain in malayaite.

In the triclinic phase the Zr atom occupies two distinct sites. In the monoclinic $A2/a$ symmetry the [ZrO_6] octahedra form linear chains parallel to [100], analogous to the high-temperature phase of $CaTiOGeO_4$ and titanite. In the triclinic form the distance between adjacent ZrO_6 chains is compressed more strongly parallel to [011] than [01$\bar{1}$], violating both the twofold screw axis and the glide plane in the $A2/a$ symmetry. As a consequence, the Zr atom

occupies symmetrically distinct positions along the octahedral chains. This asymmetric relative shift of the ZrO_6 chains is reflected by the distances between ZrO_6 chains. In the monoclinic structure the distance is the same for all Zr atoms while in the triclinic structure two distinct distances are observed.

Strain variations as a function of composition across the solid solution are expected to indicate the way in which substitution of the larger Zr atom influences the structure. Any structural or compositional change that changes the shape or volume of the octahedra must have a significant influence on any possible phase transition. The evolution of the non-symmetry breaking strain in CTGO10 and CTGO20 is, as in $CaZrOGeO_4$, in close agreement with the compound $CaTaOAlO_4$ studied by Malcherek et al. (2004). The structure of $CaTaOAlO_4$ is topologically identical with the titanite structure and it displays several displacive phase transitions. The general contraction of the titanite-framework perpendicular to the octahedral chain direction is a common feature of the transitions in CZGO and CTAO. In CZGO this contraction is accompanied by additional triclinic distortion and ensuing alteration of the other nsb-strain components e_{11} and e_{22}. Furthermore the temperature evolution of the b parameter in $CaTaOAlO_4$ only reflects thermal expansion, contrary to CTGO10 and CTGO20, which show a minor deviation in the b parameter, and as a result an additional strain expressed by the e_{22} component contributes to the scalar stain. This is probably due to the additional triclinic distortion.

The temperature evolution of the symmetry breaking strain components can be modeled using a second-order Landau-type free energy expansion. Malcherek and Bosenick (2004) described the strain evolution of $CaGe_2O_5$ using such a model. In analogy to $CaGe_2O_5$ we therefore presume that the symmetry breaking strain components e_{23} and e_{12} behave in the same manner as the order parameter for the transition, giving $e_{23} \propto e_{12} \propto Q$ as the expected strain/order parameter relationship. The symmetry breaking strain $e_4 = 2e_{23}$ is taken to be the driving order parameter of the transition, with $e_6 = 2e_{12}$ being linearly coupled to it (Carpenter and Salje 1998; Malcherek and Bosenick 2004). The solid curves in Figure 5 indicate the resulting temperature behavior

$$e_4^2 = (e_4^0)^2\left(1 - \frac{T}{T_c^*}\right)$$

Just as the temperature evolution of the symmetry breaking strain indicates a linear coupling to the order parameter of the phase transition (or its identity with the order parameter) the linear correlation between nsb-strain components and temperature indicates their coupling to the square of the order parameter (Carpenter et al. 1998).

Across the measured temperature range Rietveld refinements reveal the disordered monoclinic structure ($A2/a$) for the intermediate compounds CTGO90, CTGO80, and CTGO50. Thus the transition $P2_1/a$-$A2/a$ typical for titanite and $CaTiOGeO_4$ is not observable above ambient temperature for Zr concentrations in excess of 10% in our experiments. However, from linear extrapolation of the obtained critical temperatures the phase boundary is expected to be at 81% Ti. The addition of Zr apparently destabilizes the ordered $P2_1/a$ phase. In the ordered $P2_1/a$ phase of titanite and its analogue $CaTiOGeO_4$, the off-center vectors are oriented parallel to each other within individual octahedral chains, but antiparallel with respect to neighboring chains. In the $A2/a$ setting Ti is nominally found at the center of the $[TiO_6]$ octahedra (Speer and Gibbs 1976). The presented series of experiments reveal that replacing 10% of the octahedral Ti by Zr leads to a complete loss of the Ti out-of-center coherence. This observation is in accordance with previous findings on natural titanites, where the presence of impurities at the octahedral site leads to a similar symmetry change. Oberti et al. (1991) studied natural high-Al-titanites with $X_{Al} = Al / (Ti + Al + Fe) \geq 0.25$, using X-ray diffraction and electron microprobe analysis, and concluded that substitution of $Al(X_{Al})$ above 0.25 results in space group $A2/a$. Our observations are also in accordance with the behavior of the solid solution titanite-malayaite studied by Kunz et al. (1997). A series of experiments revealed that at a Sn concentration of 10% no $k + l$ = odd reflections could be observed, thus the addition of 10% Sn destabilizes the ordered $P2_1/a$ phase and the disordered $A2/a$ structure dominates. CTGO95 exhibits the displacive phase transition $P2_1/a$-$A2/a$ by analogy with titanite and $CaTiOGeO_4$. However, even a small Zr concentration of 5% causes lowering of the critical temperature by nearly 100 K (Fig. 8).

Despite the similar electronic properties of Zr and Ti the $P2_1/a$ phase is suppressed in $CaZrOGeO_4$, by analogy with the substitution of Ti by Sn across the titanite-malayaite join (Kunz et al. 1997).

Given the d_0-character of the Zr cation a structural distortion similar to the Ti off-centering in titanite might be expected in CZGO. The apparent absence of such an off-centering, indicated by the suppression of the $P2_1/a$-ordered phase, may be caused by the larger size of the Zr cation. The common absence of such structural distortions in Zr- and Sc-oxide compounds was discussed by Kunz and Brown (1995).

In the solid solution $(Ca_xSr_{1-x})TiOGeO_4$ substitution of the large Sr atom for Ca does not influence the transition temperature (Ellemann-Olesen and Malcherek, in preparation). However, substitution of Ge for Si at the tetrahedral site has a marked influence on T_c. The evolution of T_c with composition is nearly linear and is marked by a gradual increase of nearly 100 K from the titanite end-member toward $CaTiOGeO_4$. Therefore, the substitution of Ge for Si stabilizes the ordered $P2_1/a$ phase (Ellemann-Olesen and Malcherek 2005).

ACKNOWLEDGMENTS

Financial support through the Deutsche Forschungs-Gemeinschaft (DFG) is gratefully acknowledged. M. Kunz and E. Salje provided helpful reviews of the original manuscript.

REFERENCES CITED

Angel, R.J., Kunz, M., Miletich, R., Woodland, A.B., Koch, M., and Knoche, R.L. (1999) Effect of isovalent Si,Ti substitution on the bulk moduli of $Ca(Ti_{1-x}Si_x)SiO_5$ titanites. American Mineralogist, 84, 282–287.

Aust, H., Völlenkie, H., and Wittmann, A. (1976) Die Kristallstruktur der Hoch- und der Tieftemperaturform von $CaGe_2O_5$. Zeitschrift für Kristallographie, 144, 82–90.

Bismayer, U., Schmahl, W., Schmidt, C., and Groat, L.A. (1992) Linear birefringence and X-ray diffraction studies of the structural phase transition in titanite, $CaTiSiO_5$. Physics and Chemistry of Minerals, 19, 260–266.

Brese, N.E. and O'Keeffe, M. (1991) Bond-valence parameters for solids. Acta Crystallographica, B47, 192–197.

Carpenter, M.A. and Salje, E.K.H. (1998) Elastic anomalies in minerals due to structural phase transitions. European Journal of Mineralogy, 10, 693–812.

Carpenter, M.A., Salje, E.K.H., and Graeme-Barber, A. (1998) Spontaneous strain as a determinant of thermodynamic properties for phase transitions in minerals.

European Journal of Mineralogy, 10, 621–691.
Ellemann-Olesen, R. and Malcherek, T. (2005) A high temperature diffraction study of the solid solution $CaTiOSiO_4$–$CaTiOGeO_4$. American Mineralogist, in press.
Ghose, S., Ito, Y., and Hatch, D.M. (1991) Paraelectric-antiferroelectric phase transition in titanite, $CaTiSiO_5$: I. A high temperature X-ray diffraction study of the order parameter and transition mechanism. Physics and Chemistry of Minerals, 17, 591–603.
Groat, L.A., Raudsepp, M., Hawthorne, F.C., Ercit, T.S., Sherriff, B.L., and Hartman, J.S. (1990) The amblygonite-montebrasite series: Characterization by single-crystal structure refinement, infrared spectroscopy, and multinuclear MAS-NMR spectroscopy. American Mineralogist, 75, 992–1008.
Kek, S., Aroyo, M., Bismayer, U., Schmidt, C., Eichhorn, K., and Krane, H.G. (1997) The two-step phase transition of titanite, $CaTiSiO_5$: a synchrotron radiation study. Zeitschrift für Kristallographie, 212, 9–19.
Kunz, M. and Brown, D.I. (1995) Out-of-center distortions around octahedrally coordinated d^0 transition metals. Journal of Solid State Chemistry, 115, 395–406.
Kunz, M., Xirouchakis, D., Wang, Y., Parise, J.B., and Lindsley, D.H. (1997) Structural investigations along the join $CaTiOSiO_4$–$CaSnOSiO_4$. Schweizerisch Mineralogische Petrographische Mitteilung, 77, 1–11.
Kunz, M., Arlt, T., and Stolz, J. (2000) In situ powder diffraction study of titanite ($CaTiOSiO_4$) at high pressure and high temperature. American Mineralogist, 85, 1465–1473.
Larson, A.C. and Von Dreele, R.B. (1994) General Structure Analysis System (GSAS). Los Almos National Laboratory. Los Alamos, New Mexico.
Malcherek, T. (2001) Spontaneous strain in synthetic titanite, $CaTiOSiO_4$. Mineralogical Magazine, 65, 709–715.
Malcherek, T. and Bosenick, A. (2004) Structure and phase transition of $CaGe_2O_5$ revisited. Physics and Chemistry of Minerals, 31, 224–231.
Malcherek, T. and Ellemann-Olesen, R. (2005) CaZrGeO5 and the triclinic instability of the titanite structure type. Zeitschrift für Kristallographie, in press
Malcherek, T., Domeneghetti, C.M., Tazzoli, V., Salje, E.K.H., and Bismayer, U. (1999) A high temperature diffraction study of synthetic titanite $CaTiOSiO_4$. Phase Transitions, 69, 119–131.
Malcherek, T., Paulmann, C., Domeneghetti, M.C., and Bismayer, U. (2001). Diffuse scattering anisostropy and the $P2_1/a \leftrightarrow A2/a$ phase transition in titanite, $CaTiOSiO_4$. Journal of Applied Crystallography, 34, 108–113.
Malcherek, T., Borowski, M., and Bosenick, A. (2004) Structure and phase transitions of $CaTaOAlO_4$. Journal of Applied Crystallography, 37, 117–122.
Oberti, R., Smith, D.C., Rossi, G., and Caucia, F. (1991) The crystal chemistry of high-aluminium titanites. European Journal of Mineralogy, 3, 777–792.
Rath, S., Kunz, M., and Miletich, R. (2003) Pressure-induced phase transition in malayaite, $CaSnOSiO_4$. American Mineralogist, 88, 293–300.
Salje, E.K.H. (1990) Phase Transitions in Ferroelastic and Co-elastic Crystals. Cambridge University Press, U.K.
Salje, E.K.H., Schmidt, C., and Bismayer, U. (1993) Structural phase transition in titanite, $CaTiSiO_5$: A raman spectroscopic study. Physics and Chemistry of Minerals, 19, 502–506.
Speer, J.A. and Gibbs, G.V. (1976) The crystal structure of synthetic titanite, $CaTiOSiO_4$, and the domain textures of natural titanites. American Mineralogist, 61, 238–247.
Taylor, M. and Brown, G.E. (1976) High-temperature structural study of the $P2_1/a$-$A2/a$ phase transition in synthetic titanite, $CaTiSiO_5$. American Mineralogist, 61, 435–447.
Zhang, M., Salje, E.K.H., and Bismayer, U. (1997) Structural phase transition near 825 K in titanite: Evidence from infrared spectroscopic observations. American Mineralogist, 82, 30–35.

MANUSCRIPT RECEIVED JULY 13, 2004
MANUSCRIPT ACCEPTED SEPTEMBER 25, 2004
MANUSCRIPT HANDLED BY BRYAN C. CHAKOUMAKOS